Curie depths using combined analysis of Centroid and Matched Filtering Methods in inferring thermomagnetic characteristics of Central Brazil

Guimarães, S.N.P.[1] Ravat, D.[2] and Hamza, V.M.[1]
[1] National Observatory – ON/MCTI – Department of Geophysics
[2] University of Kentucky – UKY – Department of Earth and Environmental Sciences

This paper was prepared for presentation during the 13th International Congress of the Brazilian Geophysical Society held in Rio de Janeiro, Brazil, August 26-29, 2013.

Abstract

We use the centroid-based spectral magnetic depth determination method to determine Curie depths in central Brazil and explore their potential to examine temperature distribution in the lithosphere. Spectral matched filtering is used to cross-check the results. The results obtained have allowed us to identify primarily three principal magnetic layers in the region. The magnetic bottom/Curie depth of the sources in this region is in the range of 18-50 ±7 km. Comparison with heat flow data and results of thermal modeling suggests that the depth variations are related the characteristics of the deep thermal structure of these provinces. Comparison of the Curie depths with seismically derived Moho depths suggest that the uppermost mantle may be ferromagnetic in the central Brazilian Precambrian craton, where temperatures are at present lower than the Curie temperature.

Introduction

São Francisco and Tocantins tectonic provinces are the main structural units identified in the eastern part of the South American Platform (Almeida, 1977; Almeida et al., 1981). The areas comprising these units are collectively called the Brazilian Highlands. The São Francisco province encloses several cratonic nuclei of Archean period, whereas the age ranges of the main geologic units in the Tocantins province are Proterozoic to Archean. Results of deep seismic sounding (Franca, 2003; Assumpcao et al, 2004; Berrocal et al, 2004) in this area have been interpreted as indicating crustal thicknesses of 35 to 45 km. Heat flow values are found to fall in the range of 30 to 70 mWm^{-2} (Vitorello et al, 1980; Hamza and Muñoz, 1996; Alexandrino and Hamza, 2008).

Several airborne geophysical studies have been carried out over this region over a period from 1970 to 2005. Standard data processing techniques, discussed extensively in the literature, have been employed in analysis of aeromagnetic and aeroradiometric survey (Blum, 1999; CPRM, 2003). However, the results reported in these earlier studies provide only crude insights into the deep magnetic structure of the crust in the study area. In the present work we report progress obtained in analysis aeromagnetic data of the study area using centroid-based spectral methods (Bhattacharrya and Leu, 1975; Okubo et al, 1985) and matched bandpass filtering technique (Phillips, 2001).

Database

The aeromagnetic database available for the study area is based on results of 12 distinct airborne surveys. Standard correction procedures (including leveling and micro-leveling) and data processing techniques were applied. The map of magnetic anomaly field derived these surveys is illustrated in Figure (1).

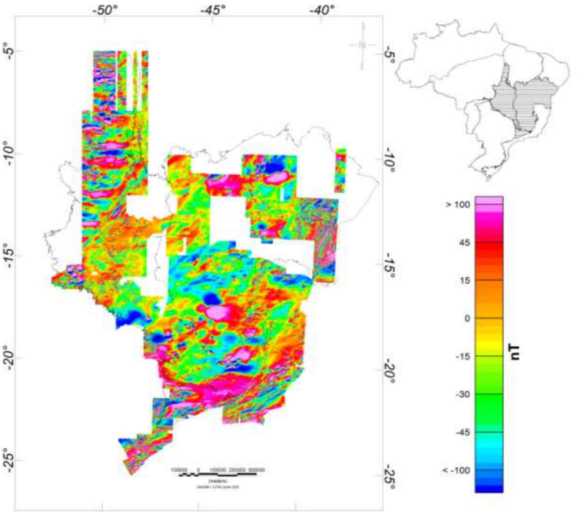

Figure (1) Crustal magnetic anomaly map of the study area.

Magnetic Depth Determination based on Spectral Methods

Several approaches have been employed in magnetic source depth determinations (Spector and Grant, 1970; Bhattacharyya and Leu, 1975; Blakely, 1995; Maus et al., 1997; Ravat et al., 2007; Bouligand et al., 2009; Bansal et al., 2011). Many of these techniques, when applied in analysis of data sets covering adequately large areas, allow the determination of the depth to bottom of magnetic layer. However, it is convenient to note that ferromagnetism may cease at certain depths either due to Curie point of magnetic minerals or petrological reasons (Wasilweski et al., 1979). An example of an amplitude spectrum of a sub-region in the study area is illustrated in Figure (2). In this figure, the lower curve is the customary amplitude spectrum whose slopes lead to the depths to the top of layers, whereas the upper one is the wavenumber-scaled amplitude spectrum whose slopes lead to determination of the centroids of the respective layers.

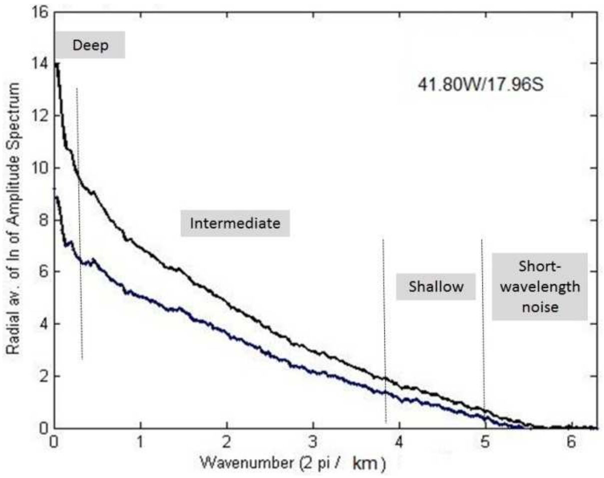

Figure (2) An example amplitude spectrum of magnetic field in the study region – using spectral slope and centroid methods.

Depths based on Fourier Amplitude Spectra and Matched Bandpass Filtering Methods

There can be many uncertainties in the determination of the depths from the radially-averaged magnetic power or amplitude spectra. In this paper, we explore the technique of matched filtering (Phillips, 1997) in verifying the results of the spectral depth computations. Matched bandpass filtering is also an effective way to separate potential-field anomalies from different magnetic layers. The method is based on the concept of idealized modeled layers below the observation surface with the chosen distribution of magnetization (e.g., a layer of dipoles or magnetic half-space). Analysis of the total field magnetic data with the matched bandpass filter extracts the wavenumbers corresponding to the principal depth ranges.

Fitting a line to the high-wavenumber end of the spectrum and removing that component separates the contribution of dipole layer from the remaining signal. Then one fits the next layer, as determined from either experimentation or the knowledge of the distribution of magnetization (i.e., layer of dipoles or a magnetic half-space) and removes its contribution. This process is continued until the steepest slope (indicating the top of deepest layer) is fit.

The values obtained for the top of these layers are then used as crosscheck for values obtained from the results of fitting slopes to the amplitude spectrum in Figure (2). Cross-checking against the model spectra from a physical model ensures that the layers in fitting the amplitude spectra are correctly identified, thus giving assurance that the centroids and bottoms estimated from the wavenumber-scaled spectra are reliable.

An example of spectra obtained by this method for the study area of the present work is illustrated in Figure (3). In this figure, the green curves represent the power spectrum while the smooth blue curve is the response to the model considered in matched filtering. In this case, the results obtained after removal of noise, is best interpreted as indicative of three layers with distinct magnetic properties.

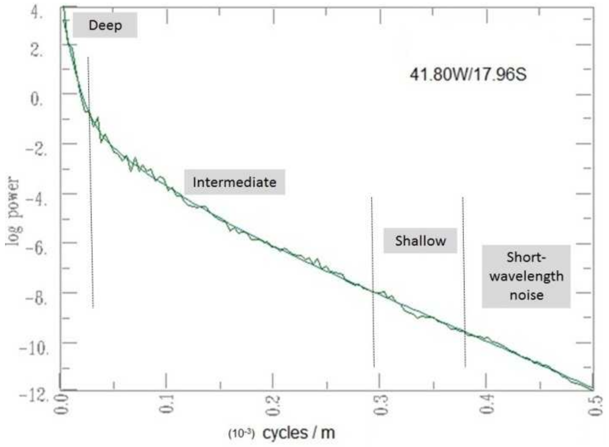

Figure (3) An example of power spectrum of magnetic field in the study region based on matched bandpass filtering.

Model Results

Calculations were carried out for total 13 overlapping gridded data sets in the study area. We tried out windows of various sizes but the results obtained with 300 km wide windows were found necessary to analyze the deepest magnetic layer. With 300 km windows size, however, only a few windows could be analyzed because of the magnetic dataset available in study. In mapping and interpreting the results, we only used those windows where the tops of layers could be corroborated by the results of the matched filtering method taking into account the usual uncertainty in derived depth (which increases steepness of the slope segment of the Fourier spectrum).

A summary of the top and the bottom depth values for each of the layers identified in the region are presented in Table (1). Comparison on the depths to top of the deepest layer obtained from the two techniques, illustrated in Figure (4), reveals reasonable agreement between the two methods used.

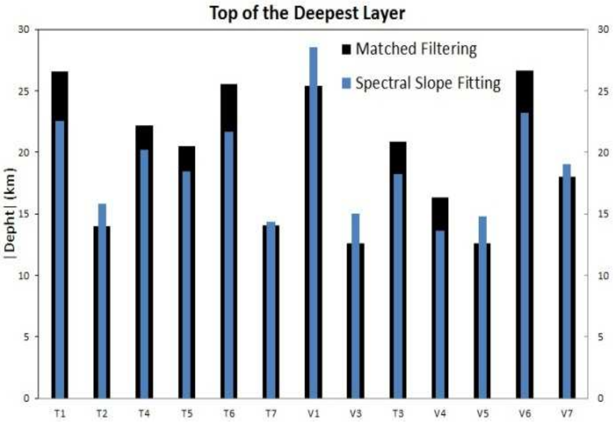

Figure (4) Comparison of values obtained from spectral slope fitting (blue) and matched filtering (black) for the top of the deepest layer of magnetic sources.

Regional Distribution of Curie Depth

The results based on the centroid method enable us to obtain the depths of the deepest sources. The regional distribution of the thickness of the magnetized crust is illustrated in the map in Figure (5). In most part of Tocantins province, the Curie depths are less than 40 km. On the other hand, the Curie depths are greater than 40 km in most parts of the São Francisco province.

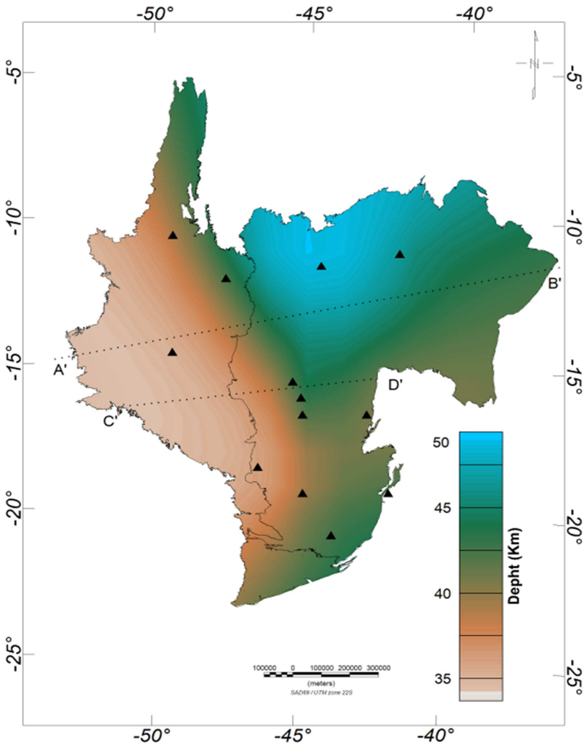

Figure (5) Map of depth to Curie isotherm (Bottom of deepest layer).

Comparison with Geothermal Data

Geothermal data are available for 204 sites in the structural provinces of Tocantins and São Francisco. The values of geothermal gradients and thermal conductivity have been used in deriving a preliminary map of surface heat flow of the study area. According to the results obtained (see Figure 6) heat flow values are systematically high in the Tocantins province compared to those in the São Francisco province.

In addition, thermal models that assume simple constant physical properties and steady state conditions have been employed in exploring the contrasts in deep thermal structures of these provinces and in estimating mantle heat flow.

According to the results obtained, the mantle heat flow is about 45 mWm^{-2} in the Tocantins province while it is less than 28 mWm^{-2} in the São Francisco province. The modeled Curie temperature (~580^{0}C) using the parameters of Table (2) are within a few km of Curie depths computed from the centroid spectral magnetic method.

Table (2) Summary of values approximate of thermal properties used in this model studies.

Structural Province	Thermal Conductivity (Wm^{-1}K^{-1})	Radiogenic Heat Production (µWm^{-3})	Heat Flow in surface (mWm^{-2})	Radiogenic Layer (km)
Tocantins	2.5	2.5	70	10
São Francisco	3.0	2.2	50	10

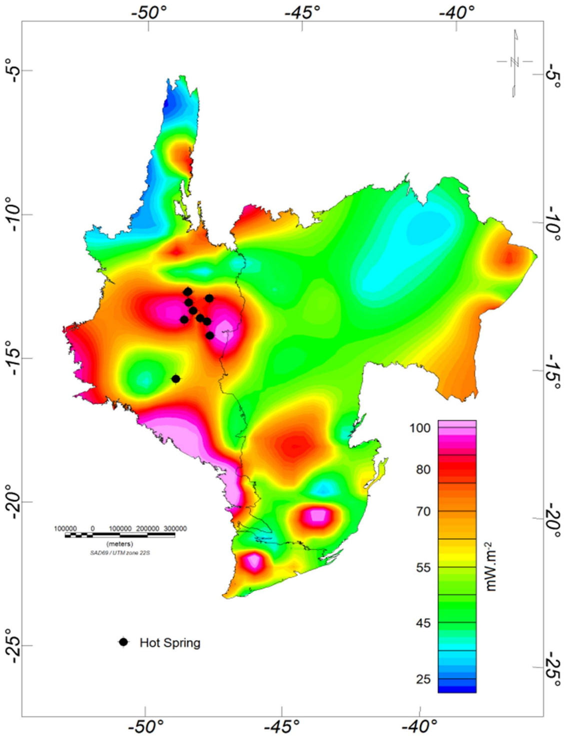

Figure (6) Map of heat flow in the study area. The dots indicate locations of main thermal spring systems.

Discussion and Conclusions

The implications of the results are best illustrated by considering the variations along west-east profiles indicated as dashed lines A'B' and C'D' in Figure (5). These profiles, presented in Figure (7), reveal that depths to Curie isotherm are around 30 km in the interior of the Tocantins province but increase to values of over 55 km in the interior of the São Francisco province. On the other hand, variations in Moho depths (Assumpcao et al, 2004; Berrocal et al, 2004) are relatively subdued, generally in the range of 35 to 40km. Consequently, the Curie isotherm is located in the lower crust in the Tocantins province whereas it is clearly in the uppermost mantle in the São Francisco province.

This latter observation is in conflict with the arguments of Wasilewski et al. (1979) and Wasilewski and Mayhew (1992) that the continental upper mantle is non-magnetic. It is possible, however, that the uppermost mantle under parts of the São Francisco Craton could be an ancient serpentinized mantle wedge similar to the modern one modeled by Blakely et al. (2005) in the Cascadia subduction margin. Recently Ravat (2012) reported magnetic bottom depths that may indicate the presence of a magnetized layer extending into the upper mantle in parts of North America. However, these results are being crosschecked, following procedures similar to those reported in the present work. Therefore, even though the cause of the ferromagnetism is not clear at this juncture, the magnetic bottom result we present here is one of the first spectral magnetic anomaly based evidence suggesting that it is possible to have ferromagnetic uppermost continental mantle where the present day temperatures are below the Curie temperature of its magnetic minerals.

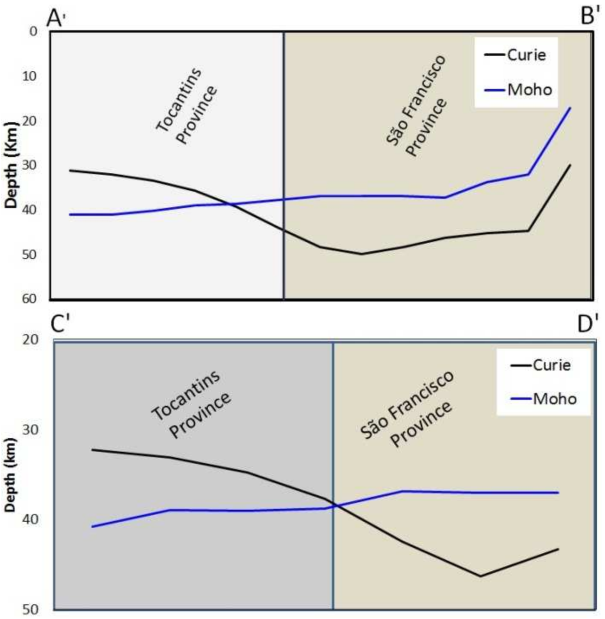

Figure (7) Crustal thicknesses and depths to Curie isotherm, along the two profiles selected in the present work.

Acknowledgements

The first author is recipient of financial support provided by CNPq – Program "Science without borders" as part of Ph.D. Sandwich (SWE) program, and was hosted by Dr. Ravat at University of Kentucky (Process: 236745/2012-3). Computer programs developed by Dr. Phillips of the U.S. Geological Survey and in the Geophysics Laboratory in the Dept. of Earth and Environmental Sciences of University of Kentucky.

References

Alexandrino, C.H. and Hamza V.M., 2008. *Estimates of heat flow and heat production and a thermal model of the São Francisco Cráton*. International Journal of Earth Sciences. v.97(2), 289-306.

Almeida, F.F.M., 1977, *O Cráton do São Francisco*. Revista Brasileira de Geociências, 7:349-364.

Almeida, F.F.M., Hasui Y., Brito Neves B.B. and Fuck, R.A., 1981, *Brazilian structural provinces: an introduction*, Earth Sci. Rev., 17: 1-19.

Assumpção, M., An, M., Bianchi, M., França, G., Rocha, M., Barbosa, J.R. and Berrocal, J. 2004. Seismic studies of the Brasília Fold Belt at the western border of the São Francisco Craton, central Brazil, using receiver function, surface wave dispersion, and teleseismic tomography. Tectonophysics, 388:173-185.

Berrocal, J., Marangoni, Y., Côgo de Sá, N.,Fuck, R.A., Soares, J.E.P., Dantas, E., Perosi, F. and Fernandes, C. 2004. *Deep seismic refraction and gravity crustal model and tectonic deformation in Tocantins Province, Central Brazil*. Tectonophysics, 388:187-199.

Bhattacharyya, B.K. and Leu, L.K. 1975. *Analysis of magnetic anomalies over Yellowstone National Park: mapping of Curie-point isothermal surface for geothermal reconnaissance*. J. Geophysics. Res., 80: 4461-4465.

Blum M. 1999. *Processamento e Interpretação de Dados de Geofísica Aérea no Brasil Central e sua aplicação à Geologia Regional e à Prospecção Mineral*. Tese (doutorado). Instituto de Geociências. Universidade de Brasília. Brasília. 229p.

Bouligand, C., Glen, J.M.G. and Blakely, R.J. 2009 *Mapping curie temperature depth in the western United States with a fractal model for crustal magnetization*. Journal of Geophysical Research. 114:B11104.

Bansal, A.R., Gabriel, G., Dimri, V.P. and Krawczyk, C.M. 2011. *Estimation of depth to the bottom of magnetic sources by a modified centroid method for fractal distribution of souces: An application to aeromagnetic data in Germany*. Gephysics. 76:L11-L22.

Blakely, R.J., 1995. *Potential Theory in Gravity and Magnetic Applications:* Cambridge University Press, London.

Blakely, R.J., Brocher, T.M. and Wells, R.E. 2005 *Subduction-zone magnetic anomalies and implications for hydrated forearc matle*. Geology. 33:445-448.

CPRM – Serviço Geológico do Brasil 2003. *Geologia, Tectônica e Recursos Minerais do Brasil: texto, mapas & SIG*, 629 p.

França, G.S.L.A. de. 2003. *Estrutura da Crosta no sudeste e centro-oeste do Brasil, usando função do receptor Local: São Paulo*. Tese (doutorado). IAG/SP 143p.

Hamza, V.M. and Muñoz, M. 1996*. Heat flow map of South America*. Geothermics. v.25. Issue 6. p.599-621 – 623-646.

Phillips, J.D., 1997, *Potential-field geophysical software for the PC, version 2.2.* U.S. Geological Survey Open-File Report 97-725.

Phillips, J.D., 2001, *Designing matched bandpass and azimuthal filters for the separation of potential-field anomalies by source region and source typ*. Australian Society of Exploration Geophysicists, 15th Geophysical Conference and Exhibition, Expanded Abstracts CD-ROM, 4p

Ravat, D., A. Pignatelli, I. Nicolosi, and M. Chiappini, 2007. *A study of spectral methods of estimating the depth to the bottom of magnetic sources from near-surface magnetic anomaly data*, Geophys. J. Int., 169, 421-434.

Ravat, D., 2012, *North American Magnetic Bottom/Curie Depth estimates and their significance for lithospheric temperature and magnetization*, (Invited), Abstract GP13C presented at 2012 Fall Meeting, AGU, San Francisco, Calif., 3-7 Dec.

Spector, A. and Grant, F.S. 1970. *Statistical models for interpreting aeromagnetic data.* Geophysics, 35(2):293-302.

Vitorello, I., Hamza, V. M. and Pollack, H. N. (1980) *Terrestrial heat flow in the Brazilian highlands*. J. Geophys. Res. v.85, 3778-3788.

Wasilewski, P.J., Thomas, H.H. and Mayhew, M.A. 1979. *The Moho as a magnetic boundary*. Geophysical Research Letters. 6:541-544.

Wasilewski, P.J. and Mayhew, M.A. (1992). *The Moho as a magnetic boundary revisited*. Geophysical Research Letters. 19:2259-2262.

Table (1) Results of the application of the two methods of delimitation of the magnetic layers.

ID	long	lat	*Centroid Method (km)*						*Matched Filtering (km)*		
			Shallow		Intermediate		Deep		Shallow	Intermediate	Deep
			TOP	BOTTOM	TOP	BOTTOM	TOP	BOTTOM	TOP	TOP	TOP
T1	-42,19	-19,32	0,73	1,15	2,27	8,02	22,53	44,31	1,22	3,29	26,54
T2	-45,03	-19,44	0,66	1,06	1,53	10,46	15,83	42,60	1,86	4,45	13,95
T4	-45,12	-16,74	0,80	1,27	1,73	18,81	20,18	53,06	1,65	3,21	22,17
T5	-44,02	-20,84	0,82	1,24	2,00	9,06	18,47	44,40	1,70	2,85	20,50
T6	-46,54	-18,59	0,74	1,27	1,82	8,07	21,64	34,52	1,37	2,61	25,55
T7	-49,4	-14,67	0,57	1,01	1,56	7,55	14,31	34,30	1,34	2,14	14,08
V1	-42,16	-11,16	1,21	1,51	2,11	12,07	28,51	47,72	1,25	2,20	25,43
V3	-49,41	-10,63	0,67	1,21	1,96	14,86	14,98	39,81	0,67	1,37	12,58
T3	-43,02	-16,67	0,69	1,13	2,18	7,13	18,22	38,26	1,98	2,35	20,83
V4	-45,47	-15,61	0,78	1,15	1,20	12,57	13,59	40,98	0,73	2,02	16,30
V5	-44,65	-11,63	0,76	2,08	3,07	6,61	14,81	56,92	0,53	1,85	12,61
V6	-47,69	-12,09	0,51	1,83	2,09	9,32	23,18	43,59	0,54	1,58	26,61
V7	-45,18	-16,16	0,84	1,37	2,10	12,27	19,02	45,78	0,57	1,97	17,99